ÖGH Herpetozoa
Austrian Herpetological Society

Herpetozoa 37: 65–72 (2024)
DOI 10.3897/herpetozoa.37.e119492

# First description of the female of *Cyrtodactylus dianxiensis* Liu & Rao, 2021, with extended diagnosis of this species (Squamata, Gekkonidae)

Dongru Zhang[1,2], Yunhe Wu[1], Changsheng Zuo[3], Fawang Yin[3], Shuo Liu[4]

1 *State Key Laboratory of Genetic Resources and Evolution, Kunming Institute of Zoology, Chinese Academy of Sciences, Kunming, Yunnan 650201, China*
2 *School of Biological Science and Technology, Liupanshui Normal University, Liupanshui, Guizhou 553004, China*
3 *Yingjiang sub-office, Tongbiguan Provincial Natural Reserve Management and Protection Bureau, Yingjiang, Yunnan 679399, China*
4 *Kunming Natural History Museum of Zoology, Kunming Institute of Zoology, Chinese Academy of Sciences, Kunming, Yunnan 650223, China*

*https://zoobank.org/B09AB19D-EE93-4F49-9F27-AA6AED129B48*

Corresponding authors: Shuo Liu (liushuo@mail.kiz.ac.cn); Yunhe Wu (yunhe2009@163.com)

Academic editor: Ben Wielstra ♦ **Received** 24 January 2024 ♦ **Accepted** 24 February 2024 ♦ **Published** 8 March 2024

## Abstract

*Cyrtodactylus dianxiensis* Liu & Rao, 2021 was originally described based on only two adult male specimens from Tongbiguan Nature Reserve, Dehong Autonomous Prefecture, western Yunnan, China. So far, no information on the females of this species is available. During comprehensive herpetofaunal investigations in 2022, one female specimen of *C. dianxiensis* was collected from Tongbiguan Nature Reserve. The female specimen agrees well with the original description of *C. dianxiensis*, and also shows some slight differences in coloration. This study reported the female specimen of this species for the first time, and provided a description and photos of the female specimen; meanwhile, we extended the diagnosis of this species.

## Key Words

bent-toed gecko, China, morphology, Yunnan

## Introduction

*Cyrtodactylus* Gray, 1827 (bent-toed geckos) is the most speciose and ecologically diverse gekkonid genus, with more than 350 recognized species distributed from the Western Himalayas through southeast Asia to the Western Pacific (Wood et al. 2012; Uetz et al. 2024). Most species of *Cyrtodactylus* are karst-adapted or granite-adapted species (Grismer et al. 2020). With the in-depth investigation of karst areas, the underestimated biodiversity of *Cyrtodactylus* has been gradually revealed (Grismer et al. 2018; Liu et al. 2021, 2023).

So far, ten species of *Cyrtodactylus* have been recognized in China, and all are distributed in southwestern China, namely Yunnan Province and Tibet Autonomous Region. Four of them were recorded in Tibet: *C. tibetanus* (Boulenger, 1905), *C. cayuensis* Li, 2007, *C. zhaoermii* Shi & Zhao, 2010 and *C. kamengensis* Mirza, Bhosale, Thackeray, Phansalkar, Sawant, Gowande, Patel & Kamengensis, 2022. The other six were recorded in Yunnan: *C. dianxiensis* Liu & Rao, 2021, *C. gulinqingensis* Liu, Li, Hou, Orlov & Ananjeva, 2021, *C. hekouensis* Zhang, Liu, Bernstein, Wang & Yuan, 2021, *C. zhenkangensis* Liu & Rao, 2021, *C. menglianensis* Liu & Rao, 2022 and *C. caixitaoi* Liu, Rao, Hou, Wang & Ananjeva, 2023, among which, *C. dianxiensis* belong to the *C. khasiensis* species group, and the remaining belong to the *C. chauquangensis* species group.

*Cyrtodactylus dianxiensis* is similar to *C. khasiensis* and previously the species have been confused with one another (Liu and Rao 2021; Wang et al. 2022). Liu and Rao (2021) describe the population of *C. khasiensis* distributed in Western Yunnan as a new species, *C. dianxiensis*. *Cyrtodactylus dianxiensis*, currently the only forest-dwelling *Cyrtodactylus* species recorded in Yunnan Province, China, was described based on one adult male holotype (KIZL2019044) from Tongbiguan Township, Yingjiang County, and one adult male paratype (KIZ2003170) from Longchuan County, both in Tongbiguan Nature Reserve, Dehong Autonomous Prefecture, western Yunnan, China (Liu and Rao 2021); no female information about this species was available. Identification verification of *C. khasiensis* voucher specimens deposited in museums could potentially yield additional specimens of *C. dianxiensis*. However, we have not yet been given the opportunity to examine the relevant specimens in other museums.

During a comprehensive herpetofaunal survey of Tongbiguan Nature Reserve in 2022, one female specimen of *Cyrtodactylus* was collected from Tongbiguan Nature Reserve, Xueli Village, Taiping Town, Yingjiang County, Dehong Prefecture, Yunnan Province, China (Fig. 1). Morphological and molecular phylogenetic analyses revealed that the specimen is *C. dianxiensis*. Here, we provide morphological data for the newly collected female specimen of *C. dianxiensis*, and extend the diagnosis of this species.

# Materials and methods

## Sampling

The specimen was sampled by hand at night. Sex was further determined based on whether the ventral side of the tail base is swollen. After euthanasia, liver tissues were taken and preserved in 95% alcohol. The specimen was then directly preserved in 75% ethanol without formalin fixation. The voucher specimen was deposited in Kunming Natural History Museum of Zoology, Kunming Institute of Zoology, Chinese Academy of Sciences (KIZ).

## Morphological analyses

The adult female specimen preserved in 75% ethanol was measured with digital calipers to the nearest 0.1 mm. Morphological terminology followed Liu and Rao (2021). Measurements included the following: snout-vent length (SVL), from tip of snout to anterior margin of cloaca; trunk length (TRL), axilla to groin distance; body width (BW), maximum width of body; tail length (TL), from posterior margin of cloaca to tip of tail; tail width (TW), maximum width of tail; head length (HL), from tip of snout to posterior margin of jaw; head width (HW), maximum width of head; head

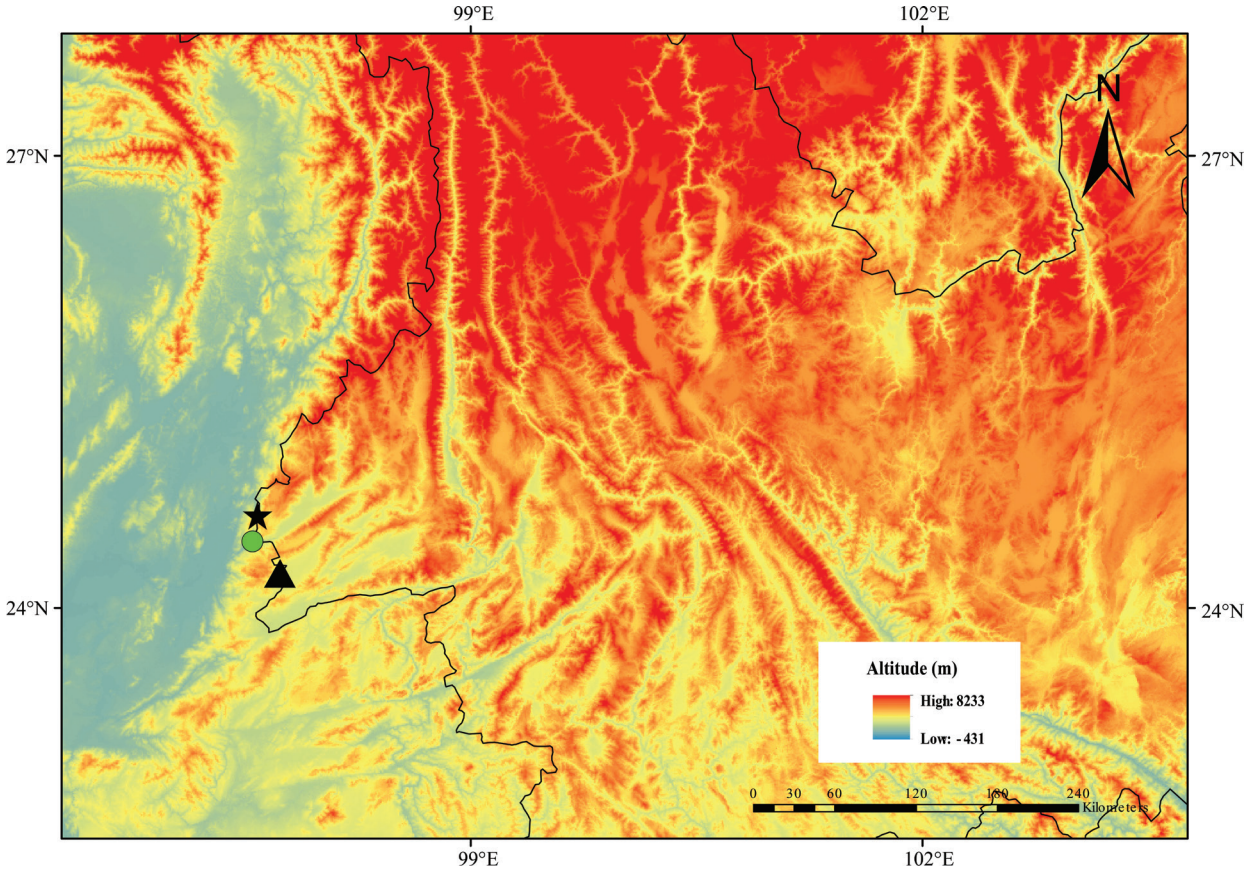


**Figure 1.** Sampling sites of *Cyrtodactylus dianxiensis*: solid black star, the locality of the holotype; solid black triangle, the locality of the paratype; solid green circle, the locality of the newly collected female specimen.

height (HH), from occiput to underside of jaws; forearm length (FL), from the base of the palm to the elbow; crus length (CL), from the base of heel to the knee; eye diameter (ED), greatest diameter of eye; nostril to eye distance (NE), from nostril to anterior corner of eye orbit; snout to eye distance (SE), from tip of snout to anterior corner of eye orbit; orbit to ear distance (EE), from posterior corner of eye orbit to anterior margin of ear opening; ear length (EL), greatest diameter of ear; internarial distance (IN), measured between inner borders of nostrils; interorbital distance (IO), measured across narrowest point of frontal bone. The counting of the following characteristics also followed Liu and Rao (2021): dorsal tubercle rows (DTR); ventral scale rows (MVSR); paravertebral tubercles (PVT); supralabials (SL); infralabials (IL); precloacal pores (PcP); precloacofemoral pores (PcFP); femoral pores on each thigh (FP); subdigital lamellae under the fourth finger (LF4) and under the fourth toe (LT4).

## DNA extraction, PCR amplification, and sequencing

Total genomic DNA was extracted from tissue samples preserved in 95% ethanol. The tissue sample was then digested using proteinase K, and subsequently purified using DNeasy Tissue Kit (QIAGEN). A fragment of NADH Dehydrogenase subunit 2 (ND2) was amplified and sequenced using the primers L4437b and H5934 (Macey et al. 1997). The experiment protocols are the same as Liu and Rao (2021). New sequence was assembled and edited using SEQMAN in Lasergene 7.1 (DNASTAR Inc., Madison, WI, USA).

## Molecular analysis

Phylogenetic relationships within the *C. khasiensis* species group were inferred from ND2. The homologous sequences of the *C. khasiensis* species group, and the outgroups species *C. slowinskii*, were downloaded from GenBank (Clark et al. 2016) (Table 1). Sequences were aligned using MUSCLE 3.6 (Edgar 2004), then checked by eye for accuracy and trimmed to minimize missing characters in MEGA 6.0.6 (Tamura et al. 2013).

Phylogenetic reconstruction was conducted using Bayesian inference (BI) and maximum likelihood (ML) methods based on the ND2 gene. The best-fit substitution model was selected under the Bayesian Information Criterion by the program MODELFINDER (Kalyaanamoorthy et al. 2017) implemented in IQ-TREE 1.6.12 (Nguyen et al. 2015). Bayesian inference analyses were performed in MRBAYES 3.2.7 (Ronquist et al. 2012) based on the model GTR+F+I+G4. Two independent runs were initiated, each with four simultaneous Markov Chain Monte Carlo (MCMC) chains for one million generations and sampled every 100 generations with a burn-in of 25%. The convergence was examined with an average standard deviation of split frequencies less than 0.01 and effective sample size (ESS) values greater than 200 in TRACER 1.5 (Rambaut and Drummond 2009). Maximum likelihood analyses were conducted using IQ-TREE 1.6.12 (Nguyen et al. 2015), based on the model TIM+F+I+G4. Nodal support was estimated by 1,000 bootstrap replicates using the ultrafast bootstrap feature. Pairwise divergences were calculated using uncorrected *p*-distances implemented in MEGA 6.0.6 (Tamura et al. 2013).

**Table 1.** Locality, voucher ID, and GenBank accession (ND2) for all samples used in this study. * denotes the holotype of *Cyrtodactylus dianxiensis*.

| Species | Locality | Voucher | Accession |
|---|---|---|---|
| *Cyrtodactylus aaronbaueri* | Mizoram, India | MZMU 2015 | MW596520 |
| *Cyrtodactylus agarwali* | Meghalaya, India | MZMU 2158 | MW596515 |
| *Cyrtodactylus arunachalensis* | Arunachal Pradesh, India | BNHS 2777 | MT341522 |
| *Cyrtodactylus aunglini* | Mandalay, Myanmar | LSUHC 13948 | MH764589 |
| *Cyrtodactylus ayeyarwadyensis* | Ayeyarwady, Myanmar | CAS 212459 | JX440526 |
| *Cyrtodactylus bapme* | Meghalaya, India | BNHS 2756 | MW367435 |
| *Cyrtodactylus bengkhuaiai* | Mizoram, India | MZMU 1985 | MW596516 |
| *Cyrtodactylus chrysopylos* | Shan State, Myanmar | LSUHC 13937 | MH764604 |
| *Cyrtodactylus dianxiensis* | Yunnan, China | KIZ059201 | MW971927 |
| *Cyrtodactylus dianxiensis* | Yunnan, China | KIZL2019044* | MW971926 |
| *Cyrtodactylus dianxiensis* | Yunnan, China | KIZ2022159 | PP394340 |
| *Cyrtodactylus exercitus* | Meghalaya, India | MZMU 2545 | OK247679 |
| *Cyrtodactylus gansi* | Chin State, Myanmar | CAS 222412 | JX440537 |
| *Cyrtodactylus guwahatiensis* | Assam, India | BNHS 2146 | KM255194 |
| *Cyrtodactylus jaintiaensis* | Meghalaya, India | BNHS 2248 | KM255195 |
| *Cyrtodactylus karsticola* | Meghalaya, India | MZMU 2156 | MW596513 |
| *Cyrtodactylus kazirangaensis* | Assam, India | BNHS 2147 | KM255170 |
| *Cyrtodactylus khasiensis* | Meghalaya, India | BNHS 2249 | KM255188 |
| *Cyrtodactylus lungleiensis* | Mizoram, India | MZMU 2428 | MZ645742 |
| *Cyrtodactylus montanus* | Tripura, India | BNHS 2231 | KM255200 |
| *Cyrtodactylus mombergi* | Kachin State, Myanmar | LSUHC 14734 | MN059875 |
| *Cyrtodactylus nagalandensis* | Nagaland, India | BNHS 2253 | KM255199 |
| *Cyrtodactylus namtiram* | Manipur, India | BNHS 2751 | MW367433 |
| *Cyrtodactylus ngopensis* | Mizoram, India | MZMU 2360 | OM912605 |
| *Cyrtodactylus septentrionalis* | Assam, India | BNHS 1989 | MH971164 |
| *Cyrtodactylus siahaensis* | Mizoram, India | MZMU 2445 | OK247677 |
| *Cyrtodactylus tripuraensis* | Tripura, India | BNHS 2238 | KM255183 |
| *Cyrtodactylus urbanus* | Assam, India | VR/ERS/ZSI/688 | MN911174 |
| *Cyrtodactylus vairengtensis* | Mizoram, India | MZMU 2903 | OP874800 |
| *Cyrtodactylus slowinskii* | Sagaing, Myanmar | CAS 210205 | JX440559 |

# Results

Bayesian inference and ML trees showed consistent topology. The newly collected female specimen clustered with the specimens (including the holotype) of *C. dianxiensis* with strong support by both BI and ML (BI/ML=1/100, Fig. 2). The genetic distance (uncorrected *p*-distance) between the newly collected female specimen and the specimens (including the holotype) of *C. dianxiensis* was only 0.9% (Table 2).

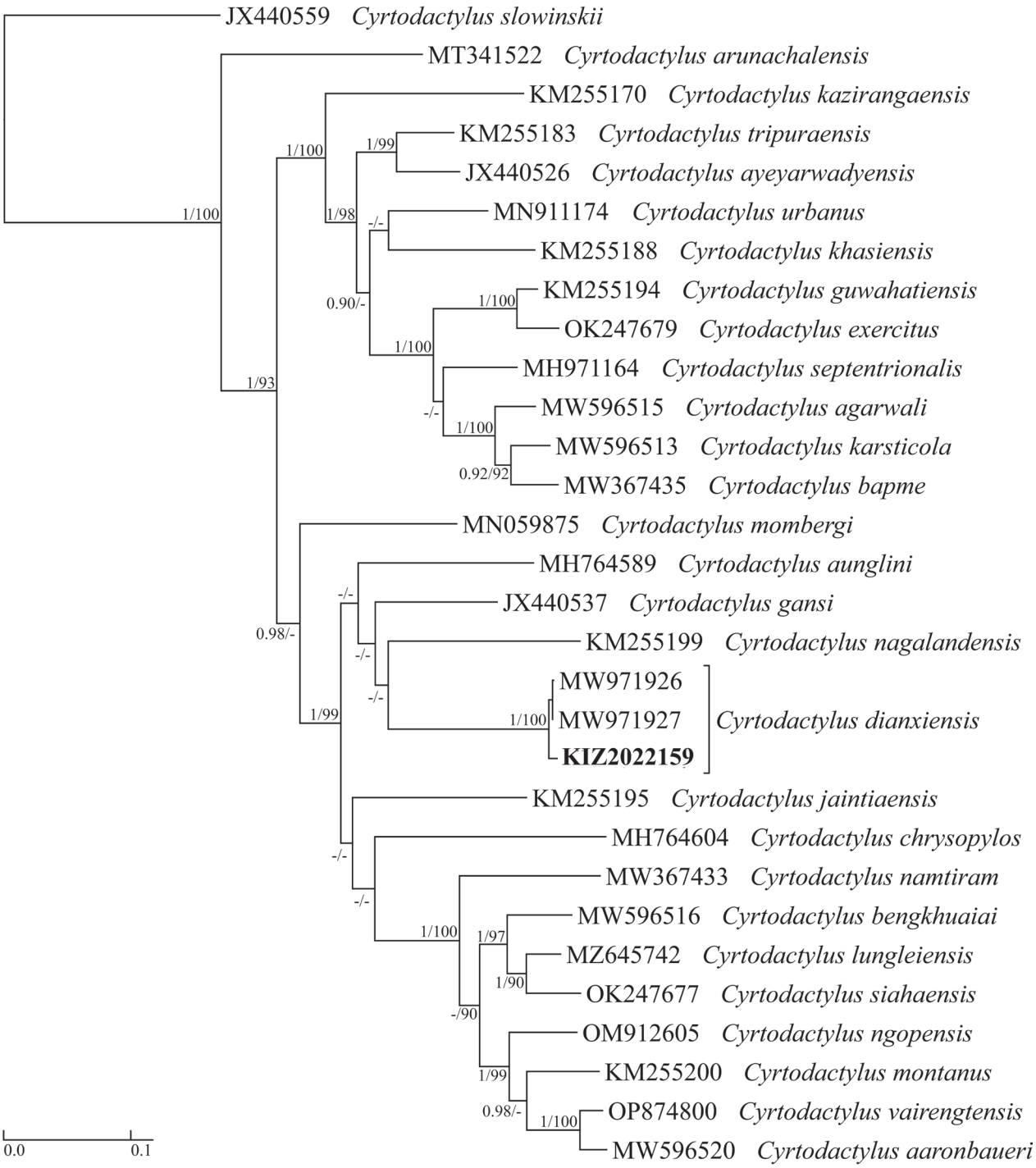


**Figure 2.** Bayesian phylogram of the *Cyrtodactylus khasiensis* species group inferred from ND2 sequences. Numbers before slashes indicate Bayesian posterior probabilities and numbers after slashes indicate the ML ultrafast bootstrap. Values below 0.90/90 are not shown.

### *Cyrtodactylus dianxiensis* Liu & Rao, 2021

Figs 3–4, Table 3

**Specimen examined.** KIZ2022159, adult female, collected on 13 September 2022 by Shuo Liu from Tongbiguan Nature Reserve, Xueli Village, Taiping Town, Yingjiang County, Dehong Prefecture, Yunnan Province, China (24°26'35"N, 97°33'1"E; at an elevation of 380 m) (Fig. 1).

**Description of the female specimen.** SVL 75.0 mm; head relatively large (HL/SVL 0.26, HW/HL 0.68), depressed (HH/HL 0.45), distinct from neck; loreal and interorbital region concave, canthus rostralis slightly swollen; snout moderately long (SE/HL 0.40); eye large (ED/HL 0.24); pupil vertical with crenulated margins; ear opening oval, obliquely oriented (EL/HL 0.08); rostral with mid-rostral suture dorsally; two large supranasals, separated by one small internasal; dorsal head scales heterogeneous,

**Table 2.** Uncorrected pairwise divergence (%) between *Cyrtodactylus khasiensis* species group members based on ND2 sequences.

| | | 1 | 2 | 3 | 4 | 5 | 6 | 7 | 8 | 9 | 10 | 11 | 12 | 13 | 14 | 15 | 16 | 17 | 18 | 19 | 20 | 21 | 22 | 23 | 24 | 25 | 26 | 27 |
|---|---|---|---|---|---|---|---|---|---|---|---|---|---|---|---|---|---|---|---|---|---|---|---|---|---|---|---|---|
| 1 | *C. aaronbaueri* | | | | | | | | | | | | | | | | | | | | | | | | | | | |
| 2 | *C. agarwali* | 24.3 | | | | | | | | | | | | | | | | | | | | | | | | | | |
| 3 | *C. arunachalensis* | 23.4 | 20.6 | | | | | | | | | | | | | | | | | | | | | | | | | |
| 4 | *C. aunglini* | 19.6 | 20.8 | 24.2 | | | | | | | | | | | | | | | | | | | | | | | | |
| 5 | *C. ayeyarwadyensis* | 21.9 | 14.8 | 20.2 | 18.2 | | | | | | | | | | | | | | | | | | | | | | | |
| 6 | *C. bapme* | 22.9 | 7.2 | 20.8 | 20.7 | 14.2 | | | | | | | | | | | | | | | | | | | | | | |
| 7 | *C. bengkhuaiai* | 12.0 | 23.6 | 20.9 | 18.3 | 19.9 | 21.9 | | | | | | | | | | | | | | | | | | | | | |
| 8 | *C. chrysopylos* | 21.7 | 21.4 | 23.1 | 18.5 | 18.9 | 21.9 | 19.2 | | | | | | | | | | | | | | | | | | | | |
| 9 | *C. dianxiensis* | 21.2 | 20.3 | 21.9 | 16.6 | 18.8 | 20.4 | 21.0 | 18.8 | | | | | | | | | | | | | | | | | | | |
| 10 | KIZ2022159 | 21.0 | 20.6 | 21.8 | 19.8 | 21.7 | 20.7 | 21.0 | 22.0 | 0.9 | | | | | | | | | | | | | | | | | | |
| 11 | *C. exercitus* | 22.5 | 11.8 | 18.4 | 21.7 | 16.2 | 13.6 | 22.5 | 21.9 | 21.3 | 21.4 | | | | | | | | | | | | | | | | | |
| 12 | *C. gansi* | 19.2 | 21.0 | 22.0 | 15.8 | 16.9 | 20.9 | 18.2 | 17.6 | 15.5 | 18.4 | 21.1 | | | | | | | | | | | | | | | | |
| 13 | *C. guwahatiensis* | 22.6 | 12.5 | 20.3 | 21.6 | 15.4 | 13.6 | 22.1 | 22.9 | 22.4 | 22.7 | 4.5 | 21.1 | | | | | | | | | | | | | | | |
| 14 | *C. jaintiaensis* | 19.2 | 23.1 | 22.9 | 19.1 | 21.8 | 22.5 | 17.3 | 22.0 | 19.1 | 19.3 | 21.4 | 19.0 | 22.4 | | | | | | | | | | | | | | |
| 15 | *C. karsticola* | 22.9 | 6.4 | 19.1 | 19.2 | 12.6 | 6.7 | 23.8 | 21.1 | 20.0 | 20.1 | 13.4 | 21.1 | 13.1 | 22.0 | | | | | | | | | | | | | |
| 16 | *C. kazirangaensis* | 24.7 | 20.0 | 21.5 | 22.5 | 16.7 | 19.6 | 22.9 | 23.7 | 21.0 | 21.3 | 18.3 | 21.7 | 19.8 | 23.0 | 17.1 | | | | | | | | | | | | |
| 17 | *C. khasiensis* | 22.7 | 17.2 | 21.0 | 21.5 | 15.6 | 16.9 | 19.5 | 22.1 | 21.9 | 22.6 | 17.0 | 20.0 | 16.9 | 21.5 | 15.2 | 18.5 | | | | | | | | | | | |
| 18 | *C. lungleiensis* | 12.1 | 21.6 | 19.9 | 18.3 | 19.2 | 20.7 | 7.2 | 20.4 | 20.3 | 19.7 | 20.2 | 18.5 | 21.1 | 18.0 | 22.0 | 21.8 | 18.8 | | | | | | | | | | |
| 19 | *C. mombergi* | 20.0 | 20.4 | 20.4 | 17.4 | 17.3 | 19.9 | 20.4 | 19.2 | 17.2 | 20.3 | 20.4 | 15.9 | 21.8 | 19.7 | 19.6 | 21.0 | 20.3 | 18.4 | | | | | | | | | |
| 20 | *C. montanus* | 10.3 | 22.9 | 22.6 | 19.6 | 20.0 | 20.5 | 12.1 | 21.5 | 19.5 | 20.1 | 20.0 | 19.6 | 21.9 | 18.8 | 22.0 | 23.3 | 21.7 | 10.9 | 19.6 | | | | | | | | |
| 21 | *C. nagalandensis* | 21.5 | 24.8 | 22.3 | 19.8 | 21.7 | 23.8 | 19.2 | 22.7 | 19.0 | 19.4 | 22.6 | 18.0 | 23.6 | 19.0 | 22.0 | 23.1 | 22.0 | 19.1 | 20.6 | 19.6 | | | | | | | |
| 22 | *C. namtiram* | 15.7 | 22.6 | 22.5 | 20.4 | 20.9 | 22.3 | 14.2 | 20.7 | 21.9 | 22.0 | 23.3 | 20.3 | 23.3 | 20.0 | 24.1 | 23.7 | 21.9 | 13.9 | 19.5 | 15.4 | 19.4 | | | | | | |
| 23 | *C. ngopensis* | 9.9 | 23.6 | 22.0 | 18.3 | 20.7 | 21.1 | 11.2 | 20.3 | 20.2 | 19.9 | 21.0 | 18.4 | 21.6 | 17.8 | 22.7 | 24.2 | 22.2 | 11.5 | 19.6 | 10.5 | 19.7 | 14.8 | | | | | |
| 24 | *C. septentrionalis* | 21.2 | 11.1 | 20.6 | 20.8 | 14.6 | 11.6 | 20.5 | 21.7 | 20.3 | 21.0 | 10.9 | 19.8 | 11.3 | 21.4 | 10.7 | 18.7 | 15.7 | 19.1 | 20.6 | 19.6 | 23.6 | 21.5 | 20.1 | | | | |
| 25 | *C. siahaensis* | 11.4 | 22.9 | 20.0 | 18.7 | 20.1 | 20.9 | 8.6 | 20.8 | 19.3 | 19.1 | 21.8 | 18.9 | 21.1 | 17.5 | 23.4 | 22.5 | 19.4 | 6.1 | 19.1 | 11.0 | 17.2 | 14.2 | 10.3 | 19.3 | | | |
| 26 | *C. tripuraensis* | 21.8 | 13.2 | 18.4 | 18.8 | 7.5 | 12.3 | 18.4 | 19.6 | 18.9 | 19.8 | 14.7 | 16.7 | 12.9 | 18.6 | 13.1 | 14.5 | 12.5 | 19.1 | 17.1 | 18.2 | 19.0 | 21.1 | 18.8 | 11.5 | 18.6 | | |
| 27 | *C. urbanus* | 23.8 | 15.6 | 20.8 | 21.3 | 13.7 | 15.1 | 21.5 | 21.5 | 20.8 | 21.1 | 14.9 | 20.0 | 15.2 | 21.8 | 14.3 | 17.3 | 14.2 | 20.1 | 20.5 | 21.8 | 22.9 | 21.6 | 21.4 | 13.4 | 20.1 | 11.5 | |
| 28 | *C. vairengtensis* | 4.0 | 24.4 | 24.2 | 18.9 | 21.1 | 22.2 | 11.2 | 21.1 | 20.8 | 20.5 | 21.9 | 18.5 | 22.2 | 18.8 | 22.3 | 24.5 | 22.8 | 11.7 | 20.4 | 10.2 | 20.1 | 15.9 | 10.3 | 20.5 | 10.6 | 20.0 | 22.3 |

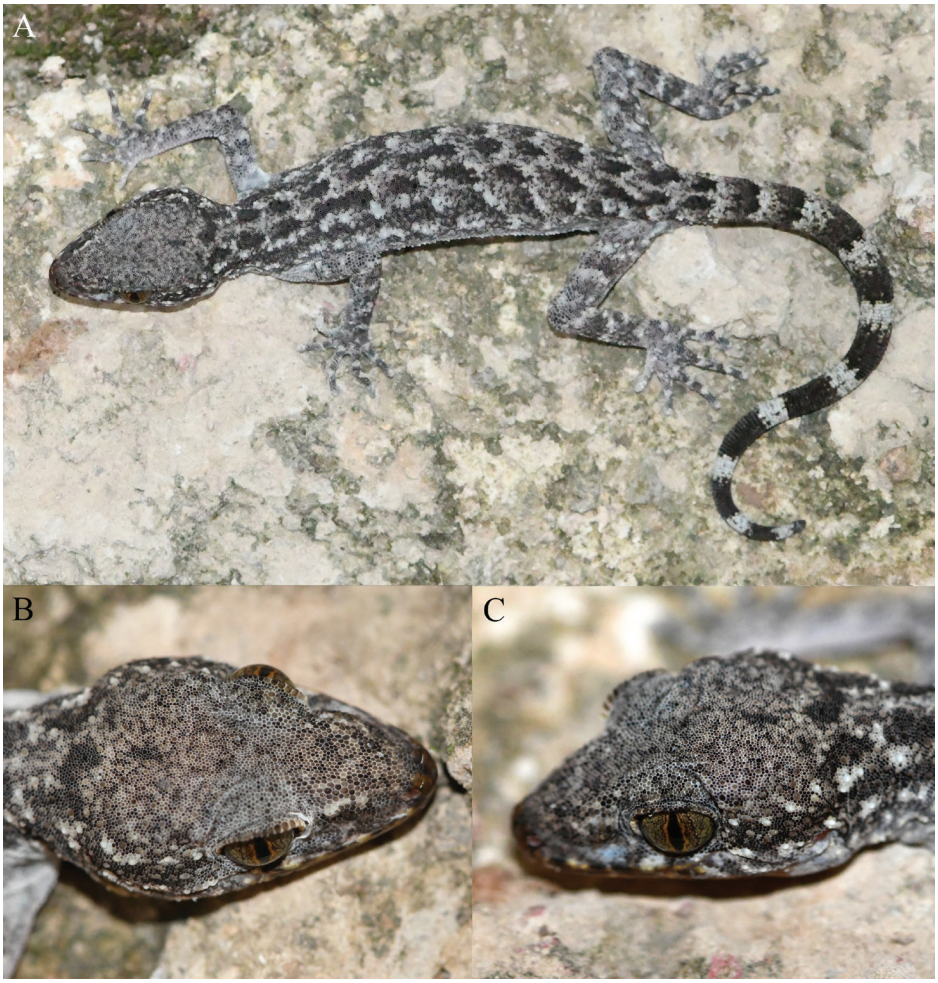


**Figure 3.** The female specimen (KIZ2022159) of *Cyrtodactylus dianxiensis* in life. **A.** Dorsal view; **B.** Close-up dorsal view of the head; **C.** Close-up dorsolateral view of the head.

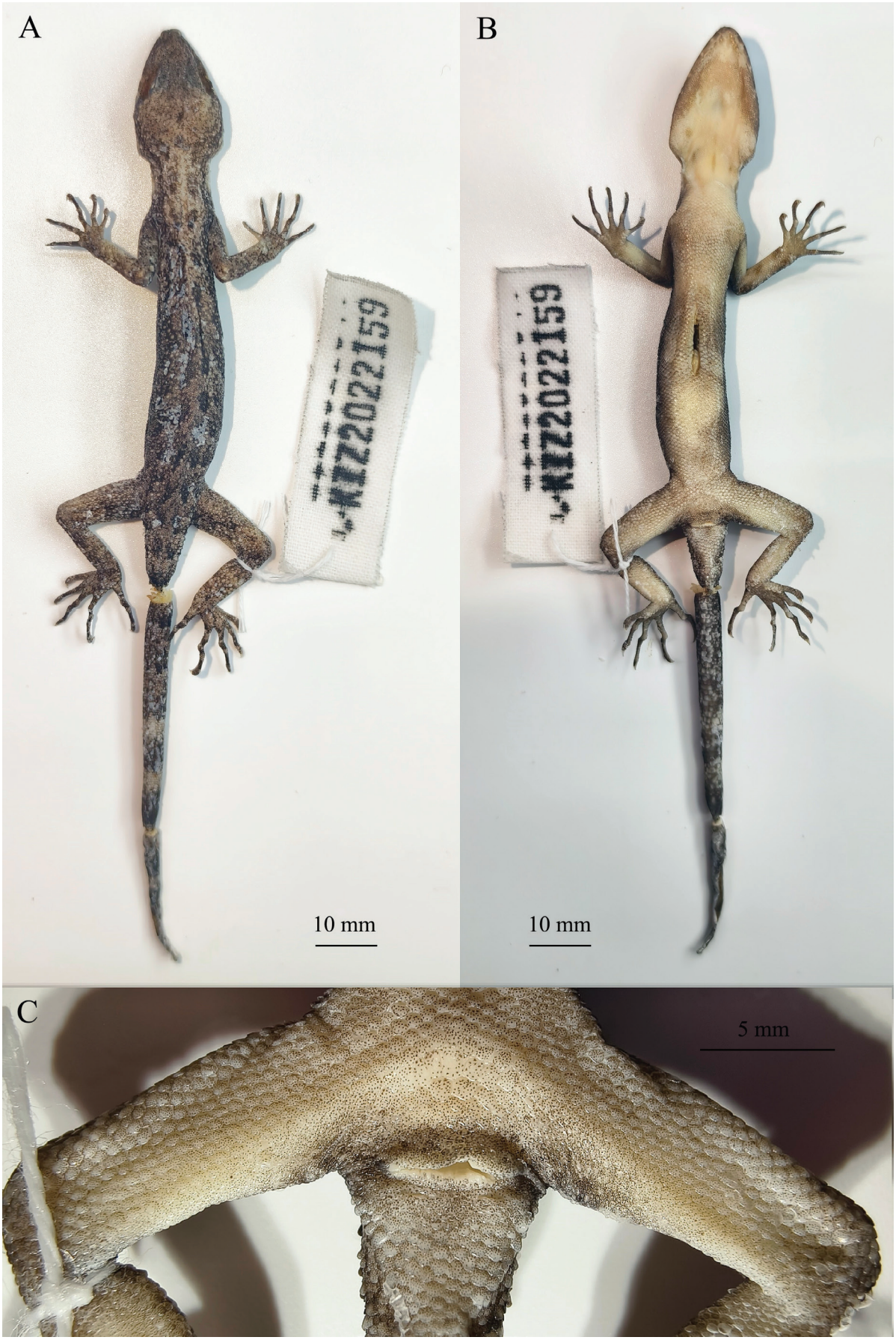


**Figure 4.** The female specimen (KIZ2022159) of *Cyrtodactylus dianxiensis* in preservative. **A.** Dorsal view; **B.** Ventral view; **C.** Close-up view of the precloacal and femoral regions.

**Table 3.** Measurements (mm) and meristic data for the female specimen of *Cyrtodactylus dianxiensis*. See Materials and methods for abbreviations.

| | KIZ2022159 | | KIZ2022159 |
|---|---|---|---|
| SVL | 75.0 | EE | 5.9 |
| TRL | 33.8 | EL | 1.6 |
| BW | 11.6 | IN | 2.5 |
| TL | 73.7 | IO | 2.6 |
| TW | 6.8 | FP | 0 |
| HL | 19.3 | PcP | 0 |
| HW | 13.2 | MVSR | 35 |
| HH | 8.6 | PVT | 32 |
| FL | 11.5 | DTR | 17 |
| CL | 13.3 | SL (R/L) | 9(7)/10(7) |
| ED | 4.6 | IL (R/L) | 9/8 |
| NE | 6.1 | LF4 | 17/16 |
| SE | 7.8 | LT4 | 20/20 |

rounded, granules; mental triangular with a pair of enlarged postmentals followed by some gradually decreasing chin-shields; scales on other region of the ventral head almost homogeneous, small, rounded, granules; supralabials seven to midorbital position on both sides, nine to angle of the jaw on right side and ten to angle of the jaw on the left side; infralabials nine on right side and seven on left side.

Body slender (TRL/SVL 0.45); dorsal scales heterogeneous, primarily small rounded granules, intermixed with irregularly arranged large circular tubercles, tubercles on nape and occipital region smaller than those on dorsum; ventrolateral folds present; ventral scales larger than dorsal; enlarged femoral scales and femoral pores absent; precloacal scales enlarged, precloacal pores absent; no precloacal groove; cloacal spurs indistinct.

Limbs slender (FL/SVL 0.15, CL/SVL 0.18); digits strongly inflected at each joint, all bearing robust, recurved claws; relative length of digits: I<II<V<III<IV (manus) and I<II<III<V<IV (pes); scales on dorsal forelimbs heterogeneous, granules, with small tubercles interspersed, scales on dorsal hind limbs heterogeneous, granular, with large conical tubercles interspersed; ventral scales of limbs almost homogeneous, granular, smaller than those on ventral body.

Original tail broken but exists, subequal to body length (TL/SVL 0.98); dorsal tail scales heterogeneous, with small tubercles interspersed; two rows of subcaudal scales slightly enlarged.

**Coloration in life.** Dorsal surface of head almost uniform brownish gray; upper lip brownish gray with many white spots, an indistinct black postorbital streak that extends backwards above ear opening on each side; a disconnected W-shaped black stripe on the occiput; dorsal surface of body brownish gray with many short black and white streaks roughly forming longitudinal rows; dorsal surface of limbs gray with indistinct white bands and spots; dorsal surface of tail grayish black with ten white bands; ventral surfaces of head, body, and limbs white, ventral surface of tail checkered with brownish gray and white; iris bronze with dark reticulations, edge of pupil orange red.

**Extended diagnosis.** Body size moderate (SVL 73.8–79.9 mm in adults); 9–12 supralabials; 8–11 infralabials; 17–19 longitudinal rows of rounded, conical dorsal tubercles; 31–32 paravertebral tubercles; 35–41 ventral scales between ventrolateral folds; no precloacal groove; femoral scales not enlarged, no femoral pores; 7–8 precloacals in males, no precloacal in female; 16–17 total subdigital lamellae beneath finger IV, 19–20 total subdigital lamellae beneath toe IV; subcaudal scales not transversely enlarged or two median rows slightly enlarged. Dorsum with light and dark blotches roughly forming longitudinal markings; a W-shaped black stripe present on occipital region; tail with 8–10 alternating dark and light bands; iris blueish gray or bronze with orange red edge.

## Discussion

The female specimen agrees well with the original description (Liu and Rao 2021) of *C. dianxiensis* in measurements and meristic counts, however, there are some slight differences in coloration between them. The female specimen has a relatively lighter body color; the dorsal head of the holotype of *C. dianxiensis* is mixed with brown and grayish white, while it is almost uniform brownish gray in the female specimen; the iris of the holotype is blueish gray with no orange red edge, while the iris is bronze with orange red edge in the female specimen. Therefore, in this species, the coloration of dorsal head is not always mottled, but may also be uniform; in addition, the iris of this species has two color types, blueish gray and bronze with orange red edge.

The holotype of *C. dianxiensis* was collected at an altitude of 1170 m and the paratype was collected at an altitude of 1200 m (Liu and Rao 2021). However, the female specimen was collected at a much lower altitude. This record extends the lowest elevational distribution of this species to 380 m.

*Cyrtodactylus dianxiensis* was previously known based on only two adult males and one juvenile (Liu and Rao 2021). This study reported the female specimen of this species for the first time, and provided a detailed description and photos of the female of this species. However, we have only collected one female specimen of this species, and it is unknown whether some differences between male and female are permanent. In addition, the range and population status of this species will need to be determined by collecting more specimens in the future.

## Acknowledgements

Thanks to the editors and reviewers for their work on the manuscript. We also would like to thank Yunnan key laboratory of biodiversity and ecological conservation of Gaoligong Mountain for its support. This

study was supported by the Science-Technology Basic Condition Platform from the Ministry of Science and Technology of the People's Republic of China (No. 2005DKA21402) and Yunnan Applied Basic Research Projects (No. 202301AT070312).

## References

Clark K, Karsch-Mizrachi I, Lipman DJ, Ostell J, Sayers EW (2016) GenBank. Nucleic Acids Research 44(D1): D67–72. https://doi.org/10.1093/nar/gkv1276

Edgar RC (2004) MUSCLE: multiple sequence alignment with high accuracy and high throughput. Nucleic Acids Research 32: 1792–1797. https://doi.org/10.1093/nar/gkh340

Grismer LL, Wood Jr. PL, Le MD, Quah ESH, Grismer JL (2020) Evolution of habitat preference in 243 species of Bent-toed geckos (Genus *Cyrtodactylus* Gray, 1827) with a discussion of karst habitat conservation. Ecology and Evolution 10: 13717–13730. https://doi.org/10.1002/ece3.6961

Grismer LL, Wood Jr PL, Thura MK, Zin T, Quah ESH, Murdoch ML, Grismer MS, Lin A, Kyaw H, Lwin N (2018) Twelve new species of *Cyrtodactylus* Gray (Squamata: Gekkonidae) from isolated limestone habitats in east-central and southern Myanmar demonstrate high localized diversity and unprecedented microendemism. Zoological Journal of the Linnean Society 182: 862–959. https://doi.org/10.1093/zoolinnean/zlx057

Kalyaanamoorthy S, Minh BQ, Wong TKF, von Haeseler A, Jermiin LS (2017) ModelFinder: fast model selection for accurate phylogenetic estimates. Nature Methods 14: 587–589. https://doi.org/10.1038/nmeth.4285

Liu S, Rao DQ (2021) A new species of *Cyrtodactylus* Gray, 1827 (Squamata: Gekkonidae) from Western Yunnan, China. Journal of Natural History 55: 713–731. https://doi.org/10.1080/00222933.2021.1921871

Liu S, Li QS, Hou M, Orlov NL, Ananjeva NB (2021) A New Species of *Cyrtodactylus* Gray, 1827 (Squamata, Gekkonidae) from Southern Yunnan, China. Russian Journal of Herpetology 28: 185–196. https://doi.org/10.30906/1026-2296-2021-28-4-185-196

Liu S, Rao DQ, Hou M, Wang QY, Ananjeva NB (2023) A new species of *Cyrtodactylus* Gray, 1827 (Squamata, Gekkonidae), previously confused with *C. wayakonei* Nguyen, Kingsada, Rösler, Auer et Ziegler, 2010. Russian Journal of Herpetology 30: 529–538. https://doi.org/10.30906/1026-2296-2023-30-6-529-538

Macey JR, Larson A, Ananjeva NB, Fang Z, Papenfuss TJ (1997) Two novel gene orders and the role of light-strand replication in rearrangement of the vertebrate mitochondrial genome. Molecular Biology and Evolution 14: 91–104. https://doi.org/10.1093/oxfordjournals.molbev.a025706

Nguyen LT, Schmidt HA, von Haeseler A, Minh BQ (2015) IQ-TREE: a fast and effective stochastic algorithm for estimating maximum-likelihood phylogenies. Molecular Biology and Evolution 32: 268–274. https://doi.org/10.1093/molbev/msu300

Rambaut A, Drummond AJ (2009) Tracer. Version 1.5. http://tree.bio.ed.ac.uk/software/tracer/

Ronquist F, Teslenko M, van der Mark P, Ayres DL, Darling A, Hohna S, Larget B, Liu L, Suchard MA, Huelsenbeck JP (2012) MrBayes 3.2: Efficient Bayesian phylogenetic inference and model choice across a large model space. Systematic Biology 61: 539–542. https://doi.org/10.1093/sysbio/sys029

Tamura K, Stecher G, Peterson D, Filipski A, Kumar S (2013) MEGA6: Molecular Evolutionary Genetics Analysis Version 6.0. Molecular Biology and Evolution 30: 2725–2729. https://doi.org/10.1093/molbev/mst197

Uetz P, Freed P, Hošek J (2024) The Reptile Database. http://www.reptile-database.org [Accessed on 24 January 2024]

Wang K, Lyu ZT, Wang J, Qi S, Che J (2022) The updated checklist and zoogeographic division of the reptilian fauna of Yunnan Province, China. Biodiversity Science 30: 21326. https://doi.org/10.17520/biods.2021326

Wood PL, Heinicke MP, Jackman TR, Bauer AM (2012) Phylogeny of bent-toed geckos (*Cyrtodactylus*) reveals a west to east pattern of diversification. Molecular Phylogenetics and Evolution 65: 992–1003. https://doi.org/10.1016/j.ympev.2012.08.025